The Photophysical and Morphological Implications of Single-Strand Conjugated Polymer Folding in Solution

Journal:	*Chemistry of Materials*
Manuscript ID	cm-2016-007343.R1
Manuscript Type:	Article
Date Submitted by the Author:	n/a
Complete List of Authors:	Fauvell, Thomas; Northwestern University, Chemistry Zheng, Tianyue; The University of Chicago, Chemistry Jackson, Nicholas; Northwestern University, Dept. of Chemistry Ratner, Mark; Northwestern University, Dept. of Chemistry Yu, Luping; University of Chicago, Chemistry Chen, Lin X.; Argonne National Laboratory, Chemical Sciences and Engineering ; Northwestern University, Chemistry

Authors are required to submit a graphic entry for the Table of Contents (TOC) that, in conjunction with the manuscript title, should give the reader a representative idea of one of the following: A key structure, reaction, equation, concept, or theorem, etc., that is discussed in the manuscript. Consult the journal's Instructions for Authors for TOC graphic specifications.

Insert Table of Contents artwork here

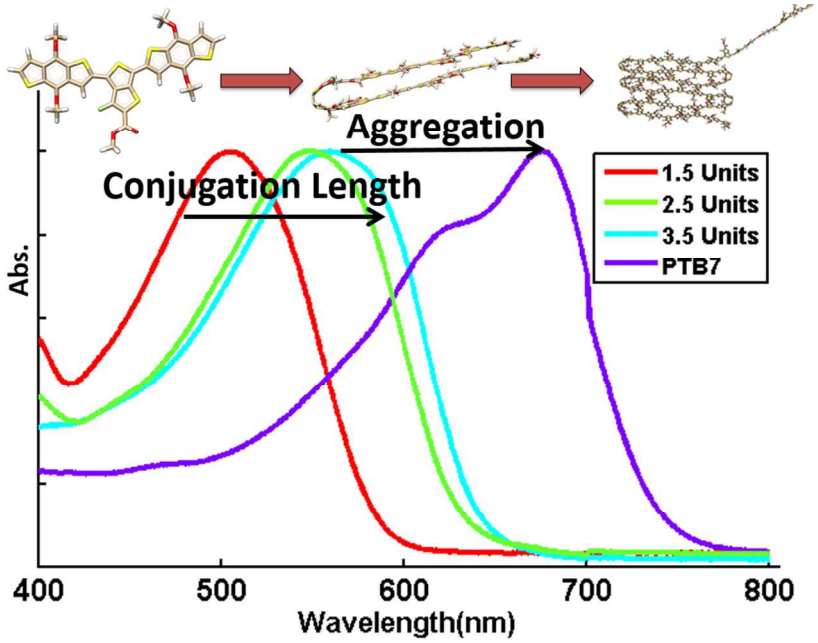

The Photophysical and Morphological Implications of Single-Strand Conjugated Polymer Folding in Solution

Thomas J. Fauvell,[†,a,b] Tianyue Zheng,[†,c] Nicholas E. Jackson, [a] Mark A. Ratner, [a] Luping Yu,[*,c] and Lin X. Chen[*,a,b]

[a]Department of Chemistry and the Argonne-Northwestern Solar Energy Research (ANSER) Center, Northwestern University, 2145 Sheridan Road, Evanston, Illinois 60208, United States

[b]Chemical Sciences and Engineering Division, Argonne National Laboratory, 9700 South Cass Avenue, Argonne, Illinois 60439, United States

[c]Department of Chemistry and Jams Frank Institute, The University of Chicago, 929 East 57th Street, Chicago, Illinois 60637, United States

ABSTRACT: Organic semiconductors have garnered substantial interest in optoelectronics, but their device performances exhibit strong dependencies on material crystallinity and packing. In an effort to understand the interactions dictating the morphological and photophysical properties of a high-performing photovoltaic polymer, **PTB7,** a series of short oligomers and low molecular weight polymers of **PTB7** were synthesized. Chain-length dependent optical studies of these oligomers demonstrate that **PTB7's** low-energy visible absorption is largely due to self-aggregation-induced ordering, rather than in-chain charge transfer, as previously thought. By examining molecular weight and concentration dependent optical properties, supplemented by molecular dynamics simulations, we attribute polymeric **PTB7's** unique mid-gap fluorescence and concentration independent absorption spectrum to an interplay between low molecular weight unaggregated strands, and high-molecular weight self-aggregated (folded) strands. Specifically, we propose that the onset of **PTB7** self-folding occurs between 7-13 repeat units, but the aggregates characteristic of polymeric **PTB7** only develop at lengths of ~30 repeat units. Atomistic molecular dynamics simulations of **PTB7** corroborate these conclusions, and a simple relation is proposed which quantifies the free-energy of conjugated polymer folding. This study provides detailed guidance in the design of intra- and inter-chain contributions to the photophysical and morphological properties of polymeric semiconductors.

INTRODUCTION

Organic semiconducting polymers have garnered interest for their numerous applications in addressing the increasing demand for affordable, lightweight, thin, flexible, and energy-efficient electronics. While extensive studies have focused on the influence of molecular structure[1,2] on both the photophysics and device performance of conjugated polymers, differentiating and controlling inter- and intra-chain contributions to optoelectronic functionality remains an elusive goal for materials scientists.[3–5] The photophysics and device performance of these soft materials have been shown to strongly depend on the electronic and geometric structures of conjugated polymers, which often drastically influence the resulting thin film morphologies[6–8] and optoelectronic properties.[9,10]

Currently, detailed correlations between molecular properties, solution aggregation structures, and the ultimate film performances of organic semiconductors are still largely unknown because of intricate and intertwined structural factors in these largely disordered and non-crystalline materials. New materials and methodologies are required to deal with the inherent complexity of soft, disordered materials.[11–15] As it stands, understanding the factors leading to the robust self-assembly of solution aggregates and their effect on various electronic processes in films following deposition is the first step towards the bottom-up design of materials with desirable bulk optoelectronic properties. Using a model system with easily manipulated solution and film properties to study the molecular factors leading to desirable bulk properties could prove crucial in beginning to unravel these connections.

While the development of low band-gap, conjugated copolymers was initially aimed at the enhancement of solar photon harvesting, especially in the NIR region, the proliferation of copolymers also induced a number of characteristics that are distinctly different from those of conventional homopolymers. For example, due to its broad, low bandgap absorption[16], favorable film morphology[7,8], efficient exciton dissociation[2,17], and, consequently, high photovoltaic performance, **PTB7** (a mono-fluorinated poly-benzodithiophenethienothiophene) has been an important material in organic photovoltaics (OPVs) research in recent years[17–19]. Studies have detailed the effects of the intra-chain "push-pull" character of its

conjugated backbone[17] on exciton binding energy in **PTB7**, but complications from possible inter-chain interactions have been largely elusive. **PTB7** also possesses somewhat unique properties as a conjugated copolymer, most notably its almost identical optical absorption spectra in dilute solution and neat film, as well as the observed decrease in photovoltaic power conversion efficiency (PCE) upon annealing in bulk heterojunction (BHJ) devices. Disentangling the effects of molecular structure and morphology will not only help optimize current **PTB7** solar cells, but will also lead to more informed design of future polymeric semiconductors.

In this report, we aim at untangling intra-chain and inter-chain electronic processes in **PTB7** by studying electronic structure evolution as a function of chain length. While computational work on chain-length dependent properties has been carried out on some conjugated polymers, [20–22] none to our knowledge has explicitly examined the critical transition of electronic processes between unfolded and folded polymeric structures in solution. Experimental work examining the length-dependent properties of oligomers has been carried out for several conjugated homopolymers which provided much useful information, [23,24] but such studies have not been utilized to examine oligomer/polymer structures in solution for conjugated copolymers. Here, a series of oligomers with different numbers of repeating units were synthesized using the same alternating electron-donating benzodithiophene (**BDT**) and electron-accepting fluorinated thienothiophene (**TT**) moieties as in **PTB7**, with the sequence (**BDT**-**TT**)$_n$-**BDT** (n=1-3) (**Scheme 1**). This series of oligomers are useful prototypes for examining photophysical properties as well as conformational changes induced by progressive chain elongation. Using these oligomers as models we utilize a combined experimental and computational approach to quantitatively probe both the photophysical effects of aggregation and the onset chain length at which intrachain aggregation occurs in **PTB7** oligomers. We hope to gain a better understanding of the hierarchical assembly of microstructural morphologies in organic electronics including bulk heterojunction organic photovoltaics.

METHODS

Synthesis of PTB7 Oligomers

Scheme 1 shows the synthetic process for the oligomers. Our previous study reported the synthesis of **M2b** by reacting **1b** with **2** at 2:1 ratio[25]. Changing the ratio to **1b:2** = 1:1, **M1** can then be synthesized. Note that there are two positions on **2** available for coupling, the 4- and the 6-position. However, from the ^{1}HNMR spectrum of **M1** (Supporting Information), only two singlet peaks (Ha and Hb) in the aromatic region are observed, indicating that there is only one isomer in the product, either 4-linkage or 6-linkage. This is further supported by the ^{19}FNMR spectrum of **M1**, which shows one singlet peak, suggesting one type of fluorine. However, it is difficult to distinguish the 4- and 6-linkage so as to identify the exact structure of **M1** at this stage, although it is possible to predict that the 6-linkage is dominant, as, according to one recent study about the similar **PTB7-Th**, 100% 6-linkage in the monomer is proposed.[26] **M2a (n=1)** is synthesized from **1a** and **2** under the same conditions as **M2b (n=1)**. However, **M2a** has free terminals that are available to be converted to the tin compound **M2c (n=1)**. Starting from **M1, M3 (n=2)** and **M4 (n=3)** are synthesized with **1c** and **M2c**, respectively. Note that in **M3** and **M4**, similar to **M1**, the fluorine atoms may face different directions, but the structures of them shown in **Figure 1** and **Scheme 1** only show one direction for clarity. This series of oligomers from **M1** to **M4** mimics the increase in molecular weight of the **PTB7** polymer chain, with the number of repeating units increasing from 1 to 3.

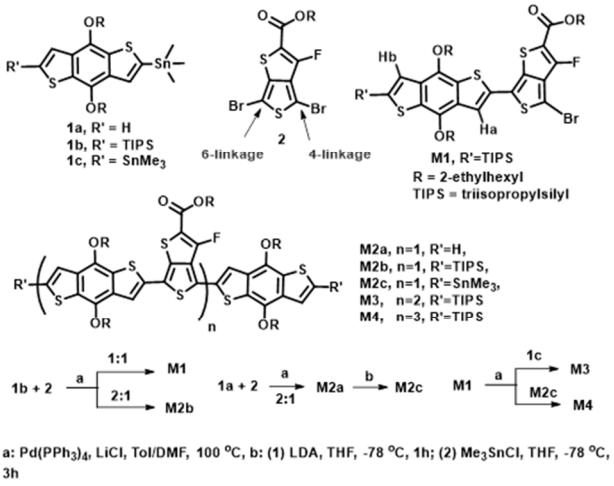

Scheme 1. Synthesis of PTB7 Oligomers

Synthesis of Low MW PTB7

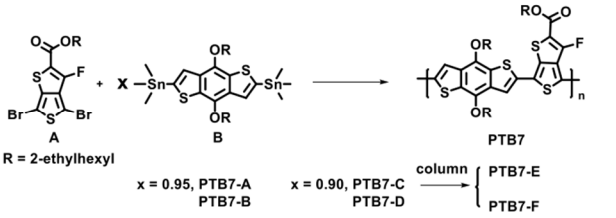

Scheme 2. Synthesis of Low Molecular Weight PTB7

In order to fill the gap between oligomeric and polymeric samples, short polymer segments were synthesized**.** Synthetic details are shown in **Scheme 2.**Molecular weights (MW) and MW distributions of polymers were determined using GPC with a Waters Associates liquid chromatography equipped with a Waters 510 HPLC pump, a Waters 410 differential refractometer and a Waters 486 tunable absorbance detector. Polystyrene was used as the standard and chloroform as the eluent. Optical properties were measured using a Shimadzu UV-

2401PC UV-Vis spectrophotometer and Shimadzu RF-5301PC spectrofluorophotometer. Scheme 2 describes the synthesis to low molecular weight PTB7.

PTB7-A and **PTB7-B**. 2-ethylhexyl-4,6-dibromo-3-fluoro thieno[3,4-*b*]thiophene-2-carboxylate (**A,** 47.0 mg, 0.0995 mmol) was weighted into a 25 ml round bottom flask together with 2,6-bis(trimethyltin)-4,8-di(2-ethylhexyloxyl) benzo [1,2-*b*:4,5-*b'*]dithiophene (**B**, 73.0 mg, 0.0945 mmol). The $Pd(PPh_3)_4$ (5.3 mg) and LiCl (0.1 mg) were added inside the glove box. The flask was vacuumized and purged with argon in three successive cycles. Then anhydrous toluene (2 ml) and DMF (0.5 ml) were injected into the mixture via a syringe. The polymerization was performed at 100°C for 24 h under argon protection. Then, 2-bromothiophene (0.03 mL) was added. After 2 hours, 2-(tributylstannyl) thiophene (0.15 mL) was added and kept overnight. A blue mixture was obtained and suction filtered through Celite to eliminate remaining palladium particles. The raw product was precipitated out in methanol and underwent Soxhlet extraction by methanol, acetone, hexane and chloroform. The final polymers were again precipitated out in methanol and dried in vacuum, yielding **PTB7-A** (36.4 mg, 50.9%) from the hexanes portion and **PTB7-B** (26.4 mg, 36.9%) from the chloroform portion. **PTB7-A**: Mn = 17.6 kDa, ~24 repeat units, Đ = 2.60. **PTB7-B**: Mn = 29.8 kDa, ~40 repeat units, Đ = 2.25.

PTB7-C ~ **PTB7-F**. Following the same procedure as for **PTB7-A** and **PTB7-B**, but with (**A**, 47.7 mg, 0.101 mmol) and (**B**, 70.2 mg, 0.0909 mmol), **PTB7-C** (34.2 mg, 49.7%) from the hexanes portion and **PTB7-D** (30.2 mg, 43.9%) from the chloroform portion were obtained. **PTB7-C**: Mn = 9.7 kDa, ~13 repeat units, Đ = 2.67. **PTB7-D**: Mn = 20.3 kDa, ~28 repeat units, Đ = 2.37. A small amount of **PTB7-C** was applied to a column chromatography on silica gel with hexanes/chloroform=1/1 as eluent to obtain the **PTB7-E** (Mn = 5.0 kDa, ~7 repeat units, Đ = 2.13) and **PTB7-F** (Mn = 16.9 kDa, ~23 repeat units, Đ = 2.37).

Spectra for Oligomers and Polymeric PTB7

UV-Visible spectra were taken on a Shimadzu UV-3600 Spectrophotometer in chloroform at low (<1mg/mL) concentration. Fluorescence spectra were taken on a Photon Technologies International model QM-2 spectrofluorimeter. Dilution spectra of PTB7 were prepared by serial dilution, heated for 5 minute to ~50°C between dilutions.

Spectra for Low Molecular Weight PTB7

UV-Visible spectra were taken by using a Shimadzu UV-2401PC UV-Vis spectrophotometer and Shimadzu RF-5301PC spectrofluorophotometer in low (<1mg/mL) concentration solution in chloroform.

Molecular Dynamics Simulations

To simulate oligomer folding in solution, molecular dynamics simulations were carried out. An atomistic force-field for PTB7 was taken from previous work where ab-initio methods were used to parameterize an all-atom OPLS-style classical force-field[10]. Periodic box sizes were chosen such that the box length > 2 times the off. Cutoffs of 10 Å and 8 Å were employed for the Lennard-Jones and Coulombic potentials, respectively, and the Particle-Particle-Particle-Mesh method was used to evaluate long-range electrostatics. Since our system is charge neutral and exhibits small atomic partial charges, we expect these specifications to be adequate. Additionally, previous work has shown that the Lennard-Jones terms dominate the electrostatic terms with regards to aggregation tendencies in these materials[10]. For each oligomer length, 50 independent trajectories were run utilizing a randomly generated regioisomer following the statistical distribution for **PTB7** recently described [26]. Each regioisomer was first optimized into a minimum energy extended state, upon which a 5-ns annealing run at 800 K occurred to access all potential energy minima, followed by a 10-ns linear cooling down to 300 K, and concluding with a 10-ns run at 300 K. Simulations utilized a Langevin thermostat with a frictional damping constant equivalent to that derived from a simple Stokes relation for chloroform (38 ps^{-1}). As we are primarily concerned with minimum energy states and not dynamics, the precise value of the frictional damping constant is not vitally important. Time evolution occurred via the velocity Verlet algorithm and the RATTLE constraint was used to constrain all bonds to Hydrogens in the system, enabling a stable 2 fs timestep. Stable folding events occurring in trajectories were catalogued for each oligomer length, from which a minimum folding length was deduced. Additional information can be found in the Supporting Information.

4.6 Quantum-Chemical Calculations

Representative aggregated and unaggregated **PTB7** tetramer structures were generated to quantify the impact of backbone flattening on the optical gap. Density-functional theory (DFT), Time-dependent density functional theory (TDDFT) and ZINDO/S calculations were performed using QCHEM and ORCA, the details of which may be found in the Supporting Information.

Simple Folding Model

A simple scaling relationship for the critical folding length of a conjugated polymer as a function of the molecular structure of its repeat unit, specifically the number of π-electrons in the repeat unit, is developed (see Supporting Information). This theory utilizes a simple treatment of the global chain motions, uncoupled dihedral degrees of freedom, and molecular dynamics input for determining the enthalpic and entropic contributions of π-π stacking interactions and kink formation to folding.

RESULTS AND DISCUSSION

Relative Contributions of Different Structural Factors on the Bandgap Narrowing in PTB7

It has been long believed that introducing the alternating electron push-pull blocks along the **PTB7** backbone is

largely responsible for lowering the optical gap of conjugated copolymers, but it has not been clear how such charge transfer character evolves as a function of the backbone length. Here structures and absorption spectra of three oligomers (**BDT-TT**)$_n$-**BDT** (n=1-3) are shown along with the corresponding polymer **PTB7** in **Figure 1**. As n increases from 1 to 2, the absorption maxima undergoes a substantial red shift of 1554 cm^{-1}, while when n changes from 2 to 3, the red-shift becomes much smaller, at 359 cm^{-1}, showing a saturation of the red shift with the oligomer length. This implies that simply extending the oligomer chain length in solution samples cannot possibly lead to the 3000 cm^{-1} red shift observed between the peak positions of the n=3 oligomer and polymeric **PTB7**. The large redshift of the polymer absorption edge relative to the oligomers is an indication that neither the increased conjugation length of the polymer, nor the molecular charge transfer character, are capable of completely accounting for **PTB7**'s narrow band gap.

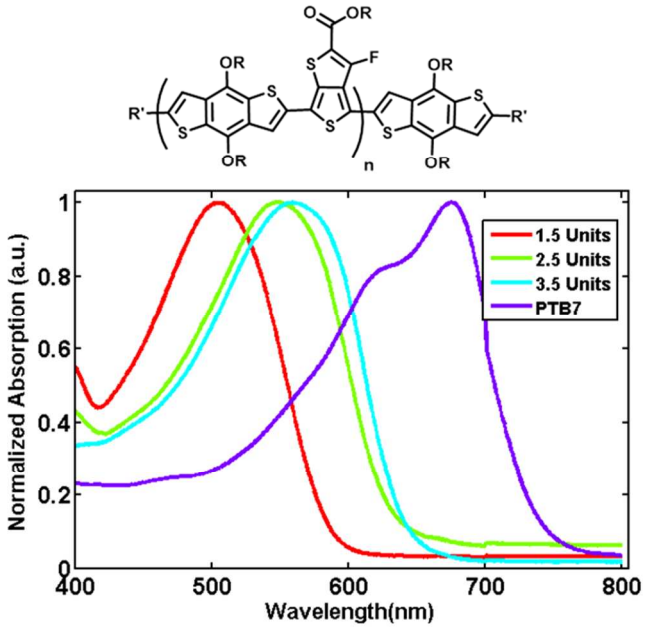

Figure 1. Top: Structure of PTB7 oligomers. Bottom: Normalized steady state solution absorption spectra. Absorption spectra are collected in dilute solution (<1mg/mL) in chloroform and normalized to a maximum abs value of 1. There is a notable red shift between n=1 and n=2 repeat units, but only a small difference between n=2 and n=3. **PTB7** has a large shift relative to all oligomers.

In order to explain the shift of the lowest energy transition band, it is worth noting the lineshape differences between the oligomers and **PTB7**. The oligomers have a smooth and featureless absorption band whereas **PTB7** shows a highly red shifted band with distinct 1500 cm^{-1} vibronic progression features. It is known in many conjugated homopolymers that the broad and featureless absorption peak is from the conformational disorder arisen from the rotations of the C-C bond connecting to adjacent blocks which generate non-planar and inhomogeneous π-conjugation. Hence, it is likely that these oligomer backbones possess various inter-repeating-unit dihedral angles (~30-40°) which are responsible for the conformational inhomogeneity and hinder π-electron delocalization.[27] In contrast, the 1500 cm^{-1} vibronic progression shown in the absorption peak of **PTB7** aligns with the conjugated C-C bond stretching frequency that can only be observed in spectra of structurally homogeneous conjugated systems, such as polythiophene in thermally annealed films, or at low temperature where conformational disorder is mitigated.[28,29] Since it is expected that electronic transitions in the oligomer absorption spectra should be mediated by the same C-C stretching mode, the comparison of the optical absorption spectral features of the oligomers and **PTB7** implies a much enhanced homogeneity in the backbone conformations of **PTB7** than in oligomers, as the dihedral degrees of freedom in the oligomers allow coexisting local conformational isomers that obscure the vibronic progression seen in the polymer. Such differences in spectral features were not observed in solution phase studies of chain length-dependent homopolymers[23,24]. A plausible explanation for both the lineshape change and the 3000 cm^{-1} redshift is the formation of ordered polymer aggregates even in dilute solution via π-π stacking, leading to planar backbone conformations with reduced structural inhomogeneity and increased intrachain and interchain electronic delocalization, including the in-chain charge transfer between adjacent electron donating **BDT** and electron withdrawing **TT** blocks. All of these factors, including differences between solution and neat-film environmental polarization effects, could contribute to such a redshift in the absorption spectrum.

To quantify the contributions of backbone planarization, excitonic coupling, and solid-state polarization to the 3000 cm^{-1} redshift, we perform quantum-chemical calculations on two geometries of a **PTB7** tetramer (Supporting Information): a geometry with all torsional angles at their energy minimized value (~30-40°), and another geometry with all torsional angles constrained to be planar. The former structure is meant to simulate **PTB7** prior to aggregation, whereas the latter is the extreme case of backbone flattening in the aggregated state. After geometry optimization of these structures we perform calculations of the lowest-lying excited state energy for the planar and non-planar geometries using a combination of semi-empirical and hybrid TDDFT methods using a continuum solvation model with a dielectric of 3. In all cases, the excited state energy redshift resulting from planarization is bounded between 1000 cm^{-1} and 1200 cm^{-1}, indicating that nearly two-thirds of the aggregation-induced redshift is the result of a combination of excitonic coupling between chromophores and solid-state polarization effects not captured by a simple continuum solvation model. The results suggest that the band gap tuning not only relies on chemical composition, but is largely determined by the chain conformation.

Preferential Folding and its Photophysical Effects

To investigate the nature of **PTB7** aggregation, concentration-dependent studies were performed as shown in **Figure 2** where very little concentration dependence of the vibronic progression was observed. At the lowest concentration (0.005mg/mL), a sphere of 14.7 nm diameter on average contains one **PTB7** chain (40kDa), whereas the average aggregate size for **PTB7** in solution is only a 3.4 - 3.7 nm diameter sphere based on solution X-ray studies at much higher concentrations[7]. Because the volume available to each **PTB7** chain is much larger than the aggregate size, it can be reasonably concluded that there are very few inter-polymer-chain interactions at this concentration. Despite this lack of interchain interaction, the vibronic fine structures are retained down to single chain levels. This is a surprising result because such a clear vibronic progression can only be observed in ordered polymers with uniform local conformations along the chain. Considering the lack of such vibrational progressions in the short oligomer spectra of **Figure 1**, our observation here seems to indicate the formation of single chain, folded self-aggregates. Furthermore, because the vibronic progression at low concentrations is not only present, but is remarkably similar to that of the higher concentration solutions, it can be concluded that **PTB7** preferentially adopts a similar conformation at all concentrations. Higher concentrations do not induce different folding patterns, but they instead contain larger multi-chain aggregates, the constituents of which are each self-folded as they are in dilute solution. This single strand folding may also explain the observation that **PTB7** has strikingly similar solution and film absorption spectra,[17] as film creation may involve simple deposition of preformed, folded structures. Additionally, these preferentially folded structures may be responsible for the fact that **PTB7's** solution structure is insensitive to solvent additives,[7] while other polymers show substantial dependencies on both concentration and additive content. [30]

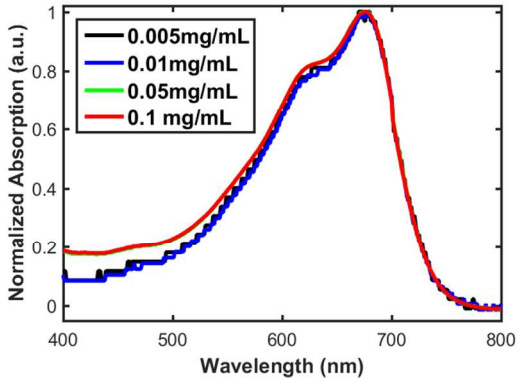

Figure 2. Normalized absorption spectra for PTB7 at different concentrations. Absorption spectra are collected in chloroform and normalized to a maximum abs value of 1. Solutions were created by serial dilution, with heating between dilutions to ensure the breakup of multi-polymer aggregates. The small changes in the vibronic features throughout the dilutions indicate that **PTB7** preferentially forms a specific folded structure within one chain. The 0.005mg/mL spectrum was close to the detection limit of the instrument.

Understanding the details of the molecular and polymeric structure leading to this powerful self-assembly of ordered structures at low concentrations is of great importance for the rational control of polymer morphologies on the nanometer scale, as it provides a means of directing the self-assembly in disordered systems at a length scale meaningful for charge and excitation transport.[31] Evidence for the specific effects of aggregation on electro-optical properties comes from noting **PTB7's** particular vibronic progression in the context of an H- or J-aggregate model[32]. The ratio of the 0-0 and 0-1 vibronic peaks in the visible absorption spectrum, being greater than 1, is suggestive of enhanced intra-chain J-aggregation via the increased polymer chain coherence lengths in these self-aggregates, which is in agreement with the large excitonic coupling induced redshift suggested from our quantum chemical calculations above. The large coherence lengths of flattened, π-stacked **PTB7** in the aggregated state are also consistent with our previous transient absorption anisotropy measurements of exciton diffusion which found **PTB7** to possess an additional sub-picosecond diffusion component compared to **P3HT**, a result which was attributed to an enhanced rigidity of **PTB7**'s backbone.[33] While **PTB7** does not form crystalline polymer films, it reliably establishes order over a meaningful local length scale that enables efficient charge transport, a fact supported by previous x-ray scattering measurements[34]. This specific, ordered self-aggregation is critical in creating order in amorphous polymer films at length scales relevant to charge and excitation transport.

Further evidence for the self-aggregation of **PTB7** is its unique mid gap solution fluorescence[35]. **Figure 3** (top) shows the absorption and fluorescence scans for **PTB7** when excited at 550nm. Exciting at the lowest energy peak (600 nm-750 nm) provides much weaker near infrared fluorescence[36]. This is expected, as many conjugated polymers exhibit behavior consistent with the red shifted, but thermally activated fluorescence of the HJ aggregate model[32,37,38]. While less intense, there is substantial absorption intensity on the blue side of the main feature. When excited in this region, at 550 nm, fluorescence is observed at energies similar to the main absorption feature. In a molecular system, this would be very strange, as internal conversion processes are typically much faster than fluorescence lifetimes, leading to fluorescence exclusively from the lowest excited state[39] appearing at lower energy in the spectral region than the lowest energy absorption peak. While it may be tempting to assign some complex energetic relaxation pathway to this observation, this fluorescence at higher energy than the lowest absorption peak is more likely due to the structural polydispersity inherent in polymers. By comparing the fluorescence spectra of the oligomers and **PTB7** in **Figure 3** (bottom),

it seems likely that this emitting species is electronically very similar to a 2.5-repeating unit oligomer.

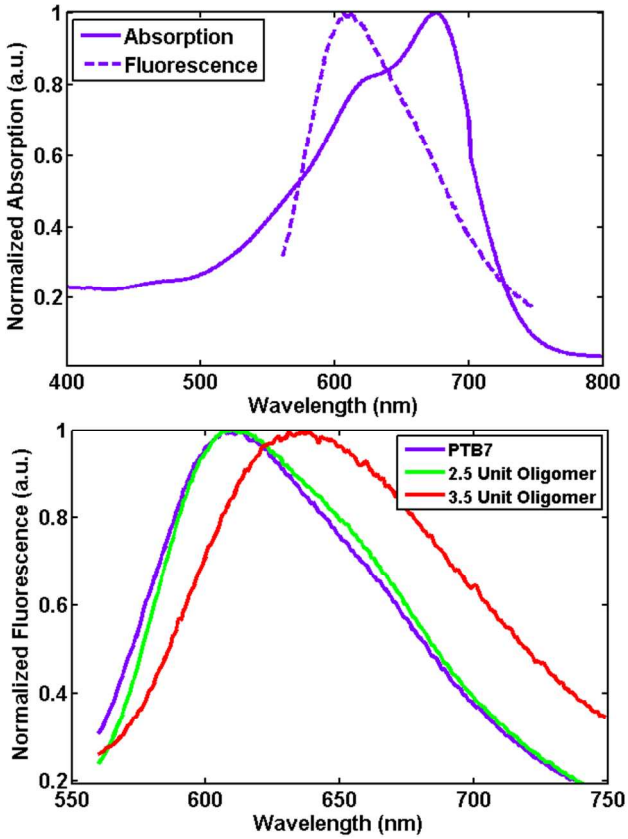

Figure 3. Absorption and fluorescence spectra of **PTB7** in chloroform (top). Fluorescence of **PTB7**, **M3** (n=2) and **M4** (n=3) (bottom). Spectra were collected at low (<1mg/mL) concentration. The fluorescence scan was excited at 550 nm. **PTB7**'s fluorescence occurs in the same spectral region as its absorption. Its fluorescence aligns with that of M3 (n=2).

Recent work from Traub et al.[4] has shown that the propensity for ordered aggregation is increased in oligomers as the lengths of the conjugated blocks are increased. Accordingly, a segment of **PTB7** on the low molecular weight (MW) end of the polydispersity curve would likely be less enthalpically favored to form ordered self-aggregates. Coupled with the previous evidence of the importance of aggregation in shifting the absorption and emission characteristics of the polymer, it can be hypothesized that the thermalized emitting species, when excited at 550 nm, is likely a smaller oligomeric segment of **PTB7,** electronically similar to **M3** (n=2), whose length is insufficient for self-folding. This effect must be seen in dilute solution, as the efficiency of this short chain fluorescence versus Förster Resonance Energy Transfer to longer, self-aggregated chains can be shown to be concentration dependent. The average distance between chains, which shifts from ~2.5nm at 1mg/mL to ~15nm at 0.005mg/mL, varies on length scales near Förster lengths common to organic molecules[40], leading to varying levels of fluorescence quenching. This argument based on Forster radii also supports the idea that the two different photophysical species do not occur on the same chain, as intrachain energy transfer processes would rapidly relax the excitation to the nearest low-energy folded segment. Similar to studies on thiophene oligomers and comparisons to polymeric **P3HT**[41], the fluorescence data seems to indicate that the size of an exciton in unaggregated **PTB7** is around two repeating units, although this should be taken with caution as the exciton's size may change within the ~100 fs[17] between its creation and subsequent localization. It is interesting that the polymer fluorescence peaked at 550 nm aligns with that of **M3** (n=2) rather than **M4** (n=3). This suggests that single strand oligomers are conformationally disordered in a fashion that prohibits the themalized exciton form delocalizing beyond two repeating units, which defines the thermalized exciton size in these copolymers/oligomers.

Using only steady state spectroscopy, it can be concluded that self-aggregation heavily affects **PTB7**'s photophysics, and is responsible for enhanced structural order and a major portion of the red shift of the bandgap.[9] These facts suggest that a single **PTB7** strand is long enough and enthalpically favored enough to form a self-folded, single chain polymeric aggregate in common solvents. Additionally, based on **PTB7**'s fluorescence spectrum it seems as though unfolded **PTB7** behaves like several connected two-repeating-unit oligomers, while the self-folded polymer behaves very differently. This self-folding fundamentally changes the photophysics of polymeric **PTB7**, and is responsible for the observed resemblance between the solution-phase and thin-film absorption spectrum of **PTB7**[17,42] the fact that **PTB7** neat films do not benefit from thermal annealing, and the need an anisotropic optical model to describe its ellipsometry[19]. Self-folding seems to create the local morphological order seen in **PTB7's** amorphous films that are critical to its unique properties. Given the conclusions of these experiments, the recent works of Traub[4], and the fact that not all conjugated polymers exhibit this behavior, it is illustrative to understand the critical molecular weight at which single chain folding is favored in **PTB7.** Moreover, for synthetic chemists seeking to make use of this powerful form of single-strand self-assembly, we seek to understand the molecular contributions to the free-energy of the folding process.

Effects of Chain Lengthening Near the Critical Folding Length

In an effort to directly observe the effects of chain lengthening near the critical folding length, a series of low molecular weight **PTB7** polymers with average chain lengths of 7, 13, 23, 28, and 40 repeating units were synthesized, as shown in **Scheme 2**, and their absorption spectra are shown in **Figure 4** (top). There are two notable trends with increasing molecular weight: an apparent red shift in absorption and a shift in the relative height of the 0-0 and 0-1 vibronic peaks. These trends can be explained by noting that the size of self-folded aggregates

should increase with increasing molecular weight. In smaller folded chains, dihedral angles can be less regular, as relatively large portions of the chain can remain unfolded. This inhomogeneity is associated with less planarity in the π system when compared to longer chains, decreasing J aggregate character, and leading to both the spectral blue shift and change in the ratio of vibronic features at lower molecular weights. A similar effect has been reported recently in temperature dependent studies of **PTB7 and PTB7-Th**[43]**.**

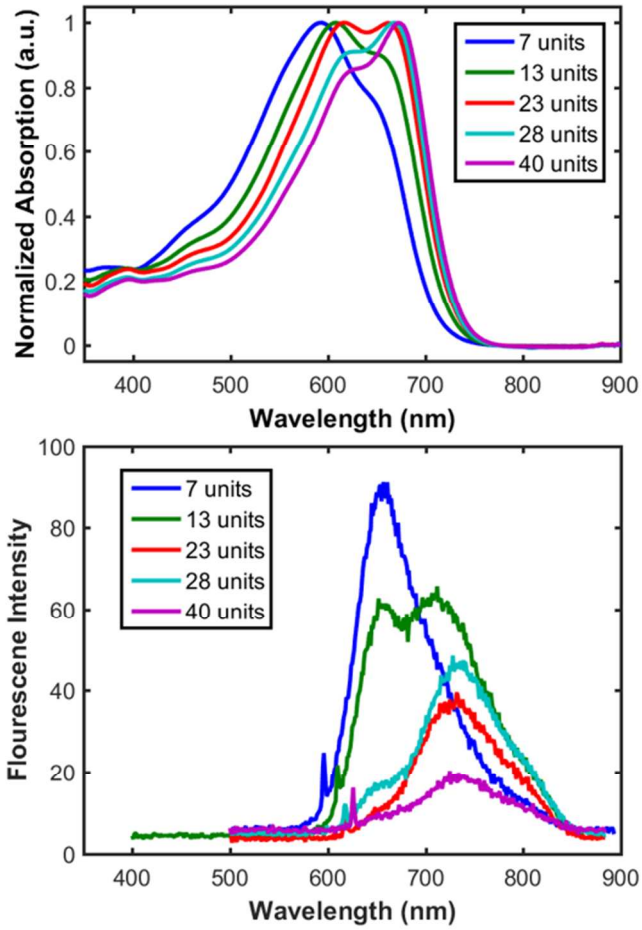

Figure 4. Normalized absorption (top) and fluorescence (bottom) spectra for PTB7 at different short polymer lengths. Absorption spectra are collected in chloroform in dilute solution (<1mg/mL) and normalized to a maximum abs value of 1. There is a noticeable red shift with increasing length, as well as a major shift in vibronic progression. Florescence spectra are collected in chloroform in dilute solution (between 0.018mg/mL and .011mg/mL) and excited in the main absorption feature (590-610nm). Concentration dependent fluorescence scans are available in the SI.

It is important to note that, because these samples were prepared by polymerization, they are inherently polydisperse. As such, any given spectrum is composed of species with varying levels of self-aggregation and its associated spectral shifts. Nonetheless, the spectral trends attributed to increasing self-folding as the average chain length increases are still apparent and are further validated by the fluorescence spectra seen in **Figure 4** (bottom), which show a length dependent change from the relatively intense **M4**-like spectrum of the 7 unit polymer to progressively more quenched **PTB7**-like fluorescence at higher molecular weights. There are two unique characteristics of the higher MW fluorescence that can be explained by two causes. First, the low fluorescence yields and the featureless spectrum of said fluorescence spectra fit the HJ aggregate model[32] that predicts a thermally activated, temperature dependent emission spectrum. Second, the emission redshift, broadening and decrease in the intensity as functions of the chain length can also fit the model for the redshifted emission from an exciton with charge transfer character, as previously observed in a series of conjugated oligomers with donor and acceptor building blocks.[48] As the self-aggregation becomes increased in longer chains, the planarization of the conjugated backbone also reinforced the charge transfer along the backbone. The displacement of the HOMO and LUMO locations along the chain will reduce the oscillator strength for the lowest energy transition, weakening the aforementioned redshifted emission. While it is predicted that an HJ aggregate should have distinct vibronic progression in its emission spectrum, the ratio of 0-0 to 0-1 features in the emission is greatly diminished at high (room) temperatures compared to lower temperatures. This, when coupled with the low quantum yield and correspondingly low signal to noise ratio, could explain the lack of distinct features. Using these data, it can be concluded that the critical length for aggregation in **PTB7** should be between 7 and 13 units, as there is a substantial shift in the peak position and shape between spectra of those samples.

Determining Energetic Contributions to Polymeric Folding

From the results of the synthesized oligomers and the low-molecular weight polymers, it is clear that folding in **PTB7** can be conservatively approximated to occur in the 4-14 repeat unit range. To enhance and verify experimental efforts in determining the critical folding length of a **PTB7** oligomer, and its molecular contributions to the free energy of this process, molecular dynamics (MD) simulations on **PTB7** oligomer lengths of n = 4, 6, 8, 10, and 12 repeat units were performed using the a Langevin thermostat in the LAMMPS simulations suite[44]. In **Figure 5** (top) we plot the fraction of trajectories resulting in a stable folded conformation as a function of oligomer length. As the critical folding length should demonstrate a solvent dependence, our simulations are an approximation to the actual critical folding length. From **Figure 5** (top) it is clear that the onset of folding occurs in the 8-10 repeat unit regime. This result is intuitively satisfying, as notions from classical polymer physics suggest that the critical length of polymer folding should be two times the Kuhn length, i.e. the length at which the chain becomes long enough to behave like an ideal chain, and the polymer is capable of folding back on itself. To our

knowledge, the persistence length of PTB7 is experimentally unknown. Given the known persistence length of P3HT as ~2-3 nm,[45] the expectation that PTB7's persistence length should be larger due to its fused π-electron system, the computational result of 8-10 units seems like a reasonable estimate for **PTB7**, and is in agreement with our experimental estimates.

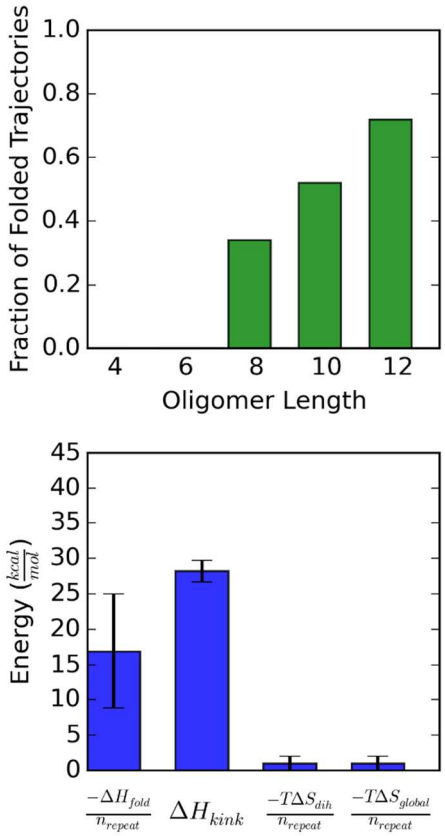

Figure 5. PTB7 Oligomer Molecular Dynamics Results. Top: Fraction of trajectories resulting in a stable, folded conformation as a function of oligomer length. Bottom: Ranges of free-energy gains and penalties associated with the folding process (see SI). The negative contributions scale with repeating units.

While these simulations do not include explicit solvent, thus representing the limiting situation of a "bad solvent", they still provide a meaningful way to quantify the enthalpic penalties and gains associated with the polymer-polymer self-interactions in the folding process in PTB7. Specifically, in **Figure 5** (bottom) we display the estimated contributions to the free energy resulting from what we hypothesize are the dominant elements. Enthalpic contributions to the folding process (polymer-polymer interaction and kink formation) are extracted from our molecular dynamics simulations, whereas simple models are used to estimate entropic terms (Supporting Information). Notably we find that the enthalpic contributions to the free energy of **PTB7** dominate the entropic contributions, especially for short chain lengths. Our estimation of the polymer-polymer interactions in **Figure 5** does not take into account the vital role of solvent contributions to the enthalpic folding process, though these forces play a vital role in making polymer folding enthalpically possible, and some estimation of the magnitudes of these contributions are available in our previous work. [10]

To make the results of this work generalizable to arbitrary conjugated polymer molecular structures, it is desirable to know, as a function of the molecular structure of a polymer, if conjugated polymer folding will be energetically allowed or not, and at what molecular weight this will occur. More importantly, we seek to provide a microscopic relation for how one should expect the propensity for chain folding to depend on the molecular identity of the conjugated backbone. Using methods described in the Supporting Information, we determine that the freezing out of dihedral degrees of freedom upon folding leads to a free energy penalty of 0.1 – 1.0 kcal/mol per repeat unit. Similarly, formation of a folded structure due to π stacking accounts for 1 kcal/mol per repeat unit entropic penalty to the free energy. Contrastingly, the enthalpic gain is approximately 16 kcal/mol per repeat unit for **PTB7**, and the enthalpic kink penalty (i.e. the energy required to form a mid-chain conformational defect which leads to folding) is ~28 kcal/mol. To this end, we advance our simple theory and predict a simple relationship for the critical folding length of a polymer as a function of the number of π electrons, demonstrating the simple inverse proportionality given by Equation 1:

$$\boldsymbol{N_{crit}} = \frac{\boldsymbol{H_{kink}(n_\pi)}}{\boldsymbol{n_\pi \alpha_\pi (\sigma_{\pi-\pi} - \sigma_{\pi-solv})}} \quad (1)$$

where N_{crit} is the critical number of repeat units of conjugated polymer required for folding, H_{kink} is the enthalpic cost of forming the kink (break in conjugation) required for folding, n_π is the number of π-electrons, α_π is a scaling factor (units = surface area), and $\sigma_{\pi\text{-}\pi}$ and $\sigma_{\pi\text{-solv}}$ are the solvation enthalpy densities of the polymer-polymer interaction and a single polymer-solvent interaction, respectively. Consequently, we hypothesize that one can expect the critical length of folding to decrease approximately inversely with the number of π-electrons present in a repeat unit. Fundamentally, the important result of Equation 1 is the fact that the critical folding length should be a ratio of the free-energy cost for kink formation to the free-energy change per repeat unit associated with the folding process; *to fold, a polymer's enthalpy change per repeat unit must be negative, and must also be larger in magnitude than the entropic penalty per repeat unit.* In theory, molecular mechanics could be used to compute both the cost of kink formation (using a short oligomer) and the free-energy change per repeat unit (using a monomer) for a given polymeric structure, enabling the rational design of mesoscale morphological properties. With enough available data on critical polymer folding lengths, one could empirically determine the value of the constant α_π in Equation 1. Future theoretical work to

rigorously describe conjugated polymer folding will benefit from the literature on coil-beta sheet transitions described previously[46,47], though such treatments are outside the scope of this work.

CONCLUSION

Using both oligomeric and low molecular weight polymeric models for **PTB7,** combined with computational analysis, the critical requirements and optical consequences of conjugated polymer folding have been deduced. Oligomeric models and their comparisons to **PTB7** show that **PTB7** forms a specific type of ordered, self-folded, self-aggregate in dilute solution, concentrated solution, and film. This is indicative of this structure forming within an isolated chain. This specific self-aggregate shows a substantial red shift in absorption relative to unfolded **PTB7,** which is shown to be oligomeric in its behavior. Notably, the coincidence of the **M3** emission with the emission of **PTB7** suggests a thermalized exciton size of approximately two repeating units in unfolded **PTB7**. In the self-aggregated **PTB7** structure, enhanced intrachain coherence lengths, implied by the HJ-aggregate like structure of the polymer, over electro-optically relevant length scales are likely largely responsible for many of the favorable properties of **PTB7.** To begin to understand the criteria for such robust self- assembly, low molecular weight polymeric models were synthesized that showed this characteristic self-aggregation occurring between 7 and 13 repeating units, confirming that longer chains are more enthalpically favored to aggregate. Theoretical considerations agreed with the approximate chain folding length and allowed for the determination of contributions to free energy for the process of self-folding. These results reveal the interplays between intra- and inter-chain interactions via polymer self-aggregation, and the importance of both in molecular design and the band gap narrowing of PTB7 and similar charge transfer copolymers.

ASSOCIATED CONTENT

Supporting Information. Thermodynamics of Conjugated Polymer Folding, MD Simulations, Quantum-Chemical Calculations, Low MW Polymer Concentration Dependent Fluorescence Spectra, Synthetic Details on **PTB7** Oligomers, HNMR Data. This material is available free of charge via the Internet at http://pubs.acs.org.

AUTHOR INFORMATION

Corresponding Author

Lin X. Chen. Email: l-chen@northwestern.edu or lchen@anl.gov

Author Contributions

†These authors contributed equally.

Funding Sources

This research was supported through the ANSER Center, an Energy Frontier Research Center funded by the U.S. Department of Energy, Office of Science, Office of Basic Energy Sciences, under Award Number DE-SC0001059 and the lab equipment was supported through the Division of Chemical Sciences, Office of Basic Energy Sciences, the U.S. Department of Energy under contract DE-AC02-06CH11357.

ACKNOWLEDGMENT

NEJ thanks Northwestern University for the award of a Presidential Fellowship.

REFERENCES

(1) Carsten, B.; Szarko, J. M.; Lu, L.; Son, H. J.; He, F.; Botros, Y. Y.; Chen, L. X.; Yu, L. Mediating Solar Cell Performance by Controlling the Internal Dipole Change in Organic Photovoltaic Polymers. *Macromolecules* **2012**, *45*, 6390–6395.

(2) Carsten, B.; Szarko, J. M.; Son, H. J.; Wang, W.; Lu, L.; He, F.; Rolczynski, B. S.; Lou, S. J.; Chen, L. X.; Yu, L. Examining the Effect of the Dipole Moment on Charge Separation in Donor-Acceptor Polymers for Organic Photovoltaic Applications. *J Am Chem Soc* **2011**, *133*, 20468–20475.

(3) Spano, F. C.; Silva, C. H- and J-Aggregate Behavior in Polymeric Semiconductors. *Annu. Rev. Phys. Chem.* **2014**, *65*, 477–500.

(4) Traub, M. C.; Dubay, K. H.; Ingle, S. E.; Zhu, X.; Plunkett, K. N.; Reichman, D. R.; Vanden Bout, D. a. Chromophore-Controlled Self-Assembly of Highly Ordered Polymer Nanostructures. *J. Phys. Chem. Lett.* **2013**, *4*, 2520–2524.

(5) Zuo, L.; Chueh, C. C.; Xu, Y. X.; Chen, K. S.; Zang, Y.; Li, C. Z.; Chen, H.; Jen, A. K. Y. Microcavity-Enhanced Light-Trapping for Highly Efficient Organic Parallel Tandem Solar Cells. *Adv. Mater.* **2014**, *26*, 6778–6784.

(6) Liu, Y.; Zhao, J.; Li, Z.; Mu, C.; Ma, W.; Hu, H.; Jiang, K.; Lin, H.; Ade, H.; Yan, H. Multiple Cases of High-Efficiency Polymer Solar Cells. *Nat. Commun.* **2014**, *5*, 1–8.

(7) Lou, S. J.; Szarko, J. M.; Xu, T.; Yu, L.; Marks, T. J.; Chen, L. X. Effects of Additives on the Morphology of Solution Phase Aggregates Formed by Active Layer Components of High-

Efficiency Organic Solar Cells. *J. Am. Chem. Soc.* **2011**, *133*, 20661–20663.

(8) Szarko, J. M.; Guo, J.; Liang, Y.; Lee, B.; Rolczynski, B. S.; Strzalka, J.; Xu, T.; Loser, S.; Marks, T. J.; Yu, L.; Chen, L. X. When Function Follows Form: Effects of Donor Copolymer Side Chains on Film Morphology and BHJ Solar Cell Performance. *Adv. Mater.* **2010**, *22*, 5468–5472.

(9) Wang, D.; Yuan, Y.; Mardiyati, Y.; Bubeck, C.; Koynov, K. From Single Chains to Aggregates, How Conjugated Polymers Behave in Dilute Solutions. *Macromolecules* **2013**, *46* , 6217–6224.

(10) Jackson, N. E.; Kohlstedt, K. L.; Savoie, B. M.; Olvera De La Cruz, M.; Schatz, G. C.; Chen, L. X.; Ratner, M. a. Conformational Order in Aggregates of Conjugated Polymers. *J. Am. Chem. Soc.* **2015**, *137*, 6254–6262.

(11) Traub, M. C.; Vogelsang, J.; Plunkett, K. N.; Nuckolls, C.; Barbara, P. F.; Vanden Bout, D. a. Unmasking Bulk Exciton Traps and Interchain Electronic Interactions with Single Conjugated Polymer Aggregates. *ACS Nano* **2012**, *6*, 523–529.

(12) Wong, C. Y.; Penwell, S. B.; Cotts, B. L.; Noriega, R.; Wu, H.; Ginsberg, N. S. Revealing Exciton Dynamics in a Small-Molecule Organic Semiconducting Film with Subdomain Transient Absorption Microscopy. *J. Phys. Chem. C* **2013**, *117*, 22111–22122.

(13) Barbour, L. W.; Hegadorn, M.; Asbury, J. B. Microscopic Inhomogeneity and Ultrafast Orientational Motion in an Organic Photovoltaic Bulk Heterojunction Thin Film Studied with 2D IR Vibrational Spectroscopy. *J. Phys. Chem. B* **2006**, *110* , 24281–24286.

(14) Tabachnyk, M.; Ehrler, B.; Gélinas, S.; Böhm, M. L.; Walker, B. J.; Musselman, K. P.; Greenham, N. C.; Friend, R. H.; Rao, A. Resonant Energy Transfer of Triplet Excitons from Pentacene to PbSe Nanocrystals. *Nat. Mater.* **2014**, *13*, 1033–1038.

(15) Niklas, J.; Mardis, K. L.; Banks, B. P.; Grooms, G. M.; Sperlich, A.; Dyakonov, V.; Beaupré, S.; Leclerc, M.; Xu, T.; Yu, L.; Poluektov, O. G. Highly-Efficient Charge Separation and Polaron Delocalization in Polymer-Fullerene Bulk-Heterojunctions: A Comparative Multi-Frequency EPR and DFT Study. *Phys. Chem. Chem. Phys.* **2013**, *15*, 9562–9574.

(16) Scharber, M. C.; Sariciftci, N. S. Efficiency of Bulk-Heterojunction Organic Solar Cells. *Prog. Polym. Sci.* **2013**, *38*, 1929–1940.

(17) Szarko, J. M.; Rolczynski, B. S.; Lou, S. J.; Xu, T.; Strzalka, J.; Marks, T. J.; Yu, L.; Chen, L. X. Photovoltaic Function and Exciton/charge Transfer Dynamics in a Highly Efficient Semiconducting Copolymer. *Adv. Funct. Mater.* **2014**, *24*, 10–26.

(18) Lu, L.; Yu, L. Understanding Low Bandgap Polymer PTB7 and Optimizing Polymer Solar Cells Based on IT. *Adv. Mater.* **2014**, *26*, 4413–4430.

(19) To, C. H.; Ng, A.; Dong, Q.; Djurišić, A. B.; Zapien, J. A.; Chan, W. K.; Surya, C. Effect of PTB7 Properties on the Performance of PTB7:PC 71 BM Solar Cells. *ACS Appl. Mater. Interfaces* **2015**, *7*, 13198–13207.

(20) Gierschner, J.; Cornil, J.; Egelhaaf, H. J. Optical Bandgaps of π-Conjugated Organic Materials at the Polymer Limit: Experiment and Theory. *Adv. Mater.* **2007**, *19*, 173–191.

(21) Zade, S. S.; Zamoshchik, N.; Bendikov, M. From Short Conjugated Oligomers to Conjugated Polymers. Lessons from Studies on Long Conjugated Oligomers. *Acc. Chem. Res.* **2011**, *44*, 14–24.

(22) Risko, C.; McGehee, M. D.; Brédas, J.-L. A Quantum-Chemical Perspective into Low Optical-Gap Polymers for Highly-Efficient Organic Solar Cells. *Chem. Sci.* **2011**, *2*, 1200.

(23) Klaerner, G.; Miller, R. D. Polyfluorene Derivatives□:

Effective Conjugation Lengths from Well-Defined. *Macromolecules* **2009**, *31*, 2007–2009.

(24) Meier, H.; Stalmach, U.; Kolshorn, H. Effective Conjugation Length and UV/vis Spectra of Oligomers. *Acta Polym.* **1997**, *48*, 379–384.

(25) Lu, L.; Zheng, T.; Xu, T.; Zhao, D.; Yu, L. Mechanistic Studies of Effect of Dispersity on the Photovoltaic Performance of PTB7 Polymer Solar Cells. *Chem. Mater.* **2015**, *27*, 537–543.

(26) Zhong, H.; Li, C. Z.; Carpenter, J.; Ade, H.; Jen, A. K. Y. Influence of Regio- and Chemoselectivity on the Properties of Fluoro-Substituted Thienothiophene and Benzodithiophene Copolymers. *J. Am. Chem. Soc.* **2015**, *137*, 7616–7619.

(27) Jackson, N. E.; Savoie, B. M.; Kohlstedt, K. L.; Olvera de la Cruz, M.; Schatz, G. C.; Chen, L. X.; Ratner, M. a. Controlling Conformations of Conjugated Polymers and Small Molecules: The Role of Nonbonding Interactions. *J. Am. Chem. Soc* **2013**, *135*, 10475–10483.

(28) Andersson, M. R.; Berggren, M.; Inganas, O.; Gustafsson, G.; Gustafssoncarlberg, J. C.; Selse, D.; Hjertberg, T.; Wennerstrom, O. Electroluminescence from Substituted Poly(thiophenes): From Blue to near-Infrared. *Macromolecules* **1995**, *28*, 7525–7529.

(29) Casado, J.; Réau, R.; Hernández, V.; Navarrete, J. T. L. Combined Raman, Electrochemical and DFT Studies on a Series of α, α□-Thiophene-Phosphole Oligomers and Their Corresponding Polymers. *Synth. Met.* **2005**, *153*, 249–252.

(30) Schmidt, K.; Tassone, C. J.; Niskala, J. R.; Yiu, A. T.; Lee, O. P.; Weiss, T. M.; Wang, C.; Fréchet, J. M. J.; Beaujuge, P. M.; Toney, M. F. A Mechanistic Understanding of Processing Additive-Induced Efficiency Enhancement in Bulk Heterojunction Organic Solar Cells. *Adv. Mater.* **2014**, *26*, 300–305.

(31) Wang, S.; Fabiano, S.; Himmelberger, S.; Puzinas, S.; Crispin, X.; Salleo, A.; Berggren, M. Experimental Evidence That Short-Range Intermolecular Aggregation Is Sufficient for Efficient Charge Transport in Conjugated Polymers. *Proc. Natl. Acad. Sci. U. S. A.* **2015**, *112*, 10599–10604.

(32) Yamagata, H.; Spano, F. C. Interplay between Intrachain and Interchain Interactions in Semiconducting Polymer Assemblies: The HJ-Aggregate Model. *J. Chem. Phys.* **2012**, *136*, 1–14.

(33) Cho, S.; Rolczynski, B. S.; Xu, T.; Yu, L.; Chen, L. X. Solution Phase Exciton Diffusion Dynamics of a Charge-Transfer Copolymer **PTB7** and a Homopolymer **P3HT**. *J. Phys. Chem. B* **2015**, *119*, 7447–7456.

(34) Hammond, M. R.; Kline, R. J.; Herzing, A. a; Richter, L. J.; Germack, D. S.; Ro, H.; Soles, C. L.; Fischer, D. a; Xu, T.; Yu, L.; Toney, M. F.; Delongchamp, D. M. Molecular Order in High-E Ffi Ciency Polymer / Fullerene Bulk Heterojunction Solar Cells. **2011**, No. 10, 8248–8257.

(35) Guo, Z.; Lee, D.; Gao, H.; Huang, L. Exciton Structure and Dynamics in Solution Aggregates of a Low-Bandgap Copolymer. *J. Phys. Chem. B* **2015**, *119*, 7666–7672.

(36) Lu, L.; Xu, T.; Chen, W.; Lee, J.; Luo, Z.; Jung, I.; Park, H.; Kim, S.; Yu, L. The Role of N □ Doped Multiwall Carbon Nanotubes in Achieving Highly E Fficient Polymer Bulk Heterojunction Solar Cells. *Nano Lett.* **2013**, *13*, 2365–2369.

(37) Jakubiak, R. Aggregation Quenching of Luminescence in Electroluminescent Conjugated Polymers. *J. Phys. Chem. A* **1999**, *103*, 2394–2398.

(38) Spano, F. C. Excitons in Conjugated Oligomer Aggregates, Films, and Crystals. *Annu. Rev. Phys. Chem.* **2006**, *57*, 217–243.

(39) Kasha, M. Characterization of Electronic Transitions in Complex Molecules. *Discuss. Faraday Soc.* **1950**, *9*, 14–19.

(40) Liu, Y. X.; Summers, M. A.; Scully, S. R.; McGehee, M. D.

Resonance Energy Transfer from Organic Chromophores to Fullerene Molecules. *J. Appl. Phys.* **2006**, *99*, 1–4.

(41) Chosrovian, H.; Rentsch, S.; Grebner, D.; Dahm, D. U.; Birckner, E.; Naarmann, H. Time-Resolved Fluorescence Studies on Thiophene Oligomers in Solution. *Synth. Met.* **1993**, *60*, 23–26.

(42) Liang, Y.; Wu, Y.; Feng, D.; Tsai, S.-T.; Son, H.-J.; Li, G.; Yu, L. Development of New Semiconducting Polymers for High Performance Solar Cells. *J. Am. Chem. Soc.* **2009**, *131*, 56–57.

(43) Bencheikh, F.; Duché, D.; Ruiz, C. M.; Simon, J. J.; Escoubas, L. Study of Optical Properties and Molecular Aggregation of Conjugated Low Band Gap Copolymers: PTB7 and PTB7-Th. *J. Phys. Chem. C* **2015**, *119*, 24643–24648.

(44) Plimpton, S. Fast Parallel Algorithms for Short – Range Molecular Dynamics. *J. Comput. Phys.* **1995**, *117*, 1–19.

(45) Cesar, B.; Rawsio, M.; Mathis, A.; Francois, B. P3Ht Persistence Length. *Synth. Met.* **1997**, *24*, 6295–6299.

(46) Hong, L. A Statistical Mechanical Model for Antiparallel Beta-Sheet/coil Equilibrium. *J. Chem. Phys.* **2008**, *129*, 1–7.

(47) Mattice, W. L.; Scheraga, H. a. Matrix Formulation of the Transition from a Statistical Coil to an Intramolecular Antiparallel Beta Sheet. *Biopolymers* **1984**, *23*, 1701–1724.

(48) Szarko, J. M.; Rolczynski, B. S.; Guo, J.; Liang, Y.; He, F.; Mara, M. W.; Yu, L.; Chen, L. X., Electronic Processes in Conjugated Diblock Oligomers Mimicking Low Band-Gap Polymers. Experimental and Theoretical Spectral Analysis. *Journal of Physical Chemistry B* **2010,** *114*, 14505-14513.